Sharp Trench Waveguide Bend with Photonic Crystals: Simulation, Fabrication and Characterization

Xudong Cui [a*], Christian Hafner [a], Franck Robin [b], Daniel Erni [c],
Kakhaber Tavzarashvili [a], Ruediger Vahldieck [a]

a. Laboratory for Electromagnetic Fields and Microwave Electronics, ETH Zurich, Switzerland
b. Electronics Laboratory, ETH Zurich, Switzerland
c. General and Theoretical Electrical Engineering (ATE), Faculty of Engineering, University of Duisburg-Essen, D-47048 Duisburg, Germany

ABSTRACT

In this paper, a three dimensional analysis of an ultra-compact sharp trench waveguide bend structure modified with small local photonic crystals is presented. The structure used here is based on a previous proposal [1]. To fully investigate the behavior of the structure, especially mode coupling and off plane radiation losses – (that are ignored in two dimensional calculations [1]) as well as the limitations caused by the effective index approximation in the two-dimensional (2D) simulations, we simulated realistic three dimensional structures using the finite integration technique. Furthermore, a structure on an InP substrate is compared with a Si/SiO2 based structure in order to check the influence of vertical index contrast on the device performance. One of the structures based on InP substrate was then fabricated and characterized to validate our conceptual predictions.

Keywords: Waveguide bends, photonic crystals, 3D simulation, effective index method, fabrication, characterization.

I. INTRODUCTION

With the development of communication technology and the increasing need for high speed network systems, device miniaturization is of a major concern, particular in future all-optical integrated circuits where high integration density is required. Waveguides and their bends as guiding medium are key components for connecting different optical devices and have a fundamental impact on the integration density. Usually when sharp bends are present in conventional waveguides, radiation losses are inevitably observed. In order to reduce the radiation losses, while keeping relatively small bend radii, new compact bend structures have been proposed in recent years [1-7]. Sensitivity Analysis has shown [1] that the required fabrication accuracy for such bends requires corner locations within accuracy of less than 20nm with respect to the optimal positions. Depending on the fabrication tolerances, this may lead to undesired failures. In order to obtain sharp waveguide bends that are less sensitive with respect to fabrication tolerances, a new concept is highly desirable.

Photonic crystals (PhCs) have attracted much attention and interest in recent years because sharp bends with zero

*xdcui@ifh.ee.ethz.ch; phone: +41 446326454

Modeling Aspects in Optical Metrology, edited by Harald Bosse, Bernd Bodermann, Richard M. Silver
Proc. of SPIE Vol. 6617, 66170D, (2007) · 0277-786X/07/$18 · doi: 10.1117/12.726017

reflection and radiation are possible in principle over a wide frequency range [7]. However, coupling of conventional waveguides with PhCs suffers from mismatching of the mode profiles of these two structures which can result in very high coupling loss. Consequently, the transition part from a conventional waveguide to PhC waveguide has to be optimized to relieve the reflection caused by such kind of impedance mismatch. This finally leaves the burden to the appropriate design and optimization. One should also keep in mind that in commonly used air-hole type PhC waveguides, the off-plane losses are high when a high index contrast material system is used.

To solve the aforementioned problems, we recently proposed a structure that combines a conventional waveguide bend with small local rod-type PhCs [1]. It was shown that high transmission and low radiation are still possible in such a structure over a wide band region, while coupling the conventional waveguide is well solved with small design efforts. For the efficient optimization of such structures, a numerical optimizer was combined with a simplified 2D model, based on the effective index method. However, these two dimensional calculation results are not reliable as good approximations of the realistic three-dimensional (3D) structure and finally, inaccuracies may guide a numerical optimization towards a sub-optimal solution. To check the effectiveness of the 2D model and to obtain information on realistic off plane radiation loss, one must at least perform 3D simulations of the most promising optimization results.

II. EFFECTIVE INDEX METHOD APPROXIMATION FOR THE WAVEGUIDE STRUCTURE DESIGN AND OPTIMIZATION

In general, it is desirable to use 3D calculations for the waveguide structure analysis because the radiation loss can then be addressed directly from full wave simulations. As a consequence, extensive computer memory and computation time are required, which cannot be accepted during the entire optimization process because usually thousands of designs need to be investigated. Therefore, one is forced to find a way to improve the computational efficiency without reducing the accuracy too much. A widely used method for waveguide computation simplification is the effective index method (EIM) approximation [8-9]. In the EIM, the 2D cross section of the 3D waveguide index profile is transformed into a one dimensional index profile, thus the 3D problems are reduced to 2D problems. A major problem of this approximation is that the EIM approach still suffers from errors in the vicinity of the cutoff [9] of any mode, even though more rigorous 2D approximation techniques are available. These techniques take the effective cladding index into account and work with an equivalent slab model [10]. For deeply etched waveguides, the applicability of this method is violated because the EIM method allows only small derivatives of the permittivity along the transversal (i.e. cross-sectional) direction while a deeply etched waveguide has a large high index contrast, i.e., when air trenches are present. Currently, one easy way to check whether the mode solver is appropriate to the actual problem or not is to examine the mode fields in the core region [8] and to see whether they are well-confined or not. This simple approach will be used throughout this paper.

The 2D cross section of our 3D trench waveguide structure is shown in Fig.1. The core layer is InGaAsP with refractive index 3.35, the top and bottom cladding layers are InP with refractive index 3.17. The substrate is n+ type InP with refractive index 3.14. The height of the top cladding, core layer, and bottom cladding layer is 200nm, 434nm, 600nm, respectively. The waveguide is deeply etched into the substrate. The whole etching depth is close to 3μm. A 2μm thickness of the substrate is used for the eigenmode calculation. In practice, the substrate would be much thicker than 2μm, but this has no severe impact on the solutions. The waveguide width is 400nm. Telecommunication wavelength 1.55μm is assumed for the following computations. Typically, the 2D equivalent waveguide exhibits two TM modes at

the wavelength 1.55μm when the central slice effective index is used when the waveguide width is 400nm [1]. We applied several eigenmode solvers [8, 11, 12] to get the effective index parameters for comparison reasons. The results are listed in table 1. Once the 2D effective index is determined, the propagation constants and field distribution of both modes are easily obtained from the eigenmode solvers.

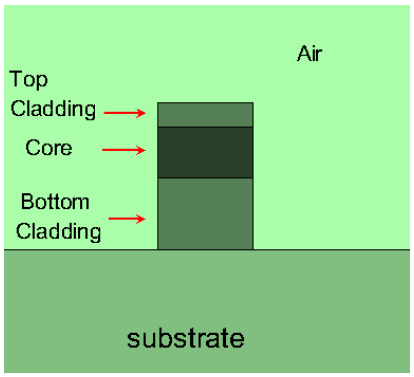

Fig.1: Schematic drawing of the 2D cross section of the deeply etched waveguide.

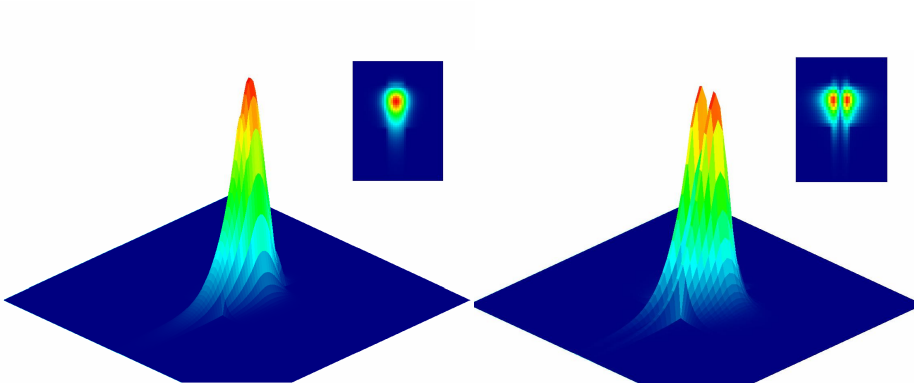

(a) (b)

Fig.2: Eigenmode profiles of the fundamental mode and the second mode that can propagate in the InP trench waveguide, red colors indicate high field values. Inset: main plot in 2D cross section; (a) Surface plot of the optical field of the fundamental mode at 1.55μm; (b) The second mode.

Table 1: Calculated effective index from different eigenmode solvers for the fundamental TM mode of InP trench waveguide at 1.55 μm.

Eigenmode Solver	2D Effective index	1-D central slice effective index	1-D lateral slice effective index	Propagation Constant
Hammer EIM [8]	3.160	3.230	1.000	12.800 μm^{-1}
Apollo [11]	2.918	3.213	1.0595	11.828 μm^{-1}
MWS [12]	2.906	/	/	11.780 μm^{-1}

As we can see from table 1, the results of the different solvers exhibit some differences. This may cause confusion since we are not sure which solver is most accurate. Selecting the best approximation is also important because an inaccurate field solver might guide the numerical optimizer towards a useless or at least sub-optimal solution. Furthermore, inaccuracies may cause noise in the fitness evaluation which may considerably slow down the optimization process. As a compromise, we select n = 3.23 as the effective index of the central slice for our bend design in 2D. Afterwards, the geometry parameters obtained from two dimensional optimizations are used for the 3D simulation [1]. It's worth mentioning that the waveguide operates in dual mode regime. This makes the fitness definition and the field analysis more tricky than for single mode waveguides. Within our earlier 2D optimization of the bend structure the fitness function was defined in such a way that the transmission coefficient of the fundamental mode is maximized. This simple fitness definition implies simultaneously low radiation, low reflection, and low mode conversion [1]. However, one certainly cannot say before the optimization is performed whether it is possible to find a solution with simultaneously low radiation, low reflection, and low mode conversion.

III. 3D SIMULATION OF AN InP/InGaAsP MATERIAL BASED TRENCH WAVEGUIDE

An optimized 3D trench waveguide bend is shown in Fig.3a and the corresponding geometric parameters can be found in [1]. To save computation time, the substrate is not included in the calculation (Note that this may lead to differences in the results due to the weak vertical confinement of the waveguide). The commercial software package CST Microwave Studio® (MWS) - based on the Finite Integration Technique (FIT) [12] - was chosen for the 3D analysis. What we have to do first is to determine the modes that can propagate in the structure. Therefore, the mode matching technique is preferred for waveguide structure modeling because this technique assumes that the portion of the input waveguide mode incident upon it is completely transmitted through the waveguide and the reflection of the mode at the input port is small. This is a very important step for the accurate computation because mismatching at the waveguide ports causes spurious reflection and incorrect losses. It is important to note that there is no direct waveguide port setting for the dielectric waveguide simulation in MWS. The waveguide ports in MWS are shielded by a perfect electrical conductor (PEC) and the associated eigenmodes are limited to a well-determined area in the port region. Therefore, one has to define a sufficiently large area that covers the in-coupling waveguide region as the port to have to encompass the dielectric waveguide modes.

Obviously, the waveguide port setting in the simulation is a compromise, based on the fact that the higher the frequency, the more field is concentrated in the dielectric with highest refractive index for the inhomogeneous waveguide port. This is clearly seen in Fig.3b. As a matter of fact, mode mismatching always exists when using MWS for dielectric waveguide structures. A difference with other mode solvers is that the effective area of the mode is larger than that of the results shown in Fig.2. One appropriate port region was found by further increasing the cover region at the port until the mode profile and propagation constant did not change anymore.

After solving the excitation problem in MWS, we investigated the radiation losses, which in fact depend on the behavior of the field far away from the core. Therefore, we check the field distribution in the central planes of the three waveguide layers. The cutting planes are parallel to *xy* plane as indicated in Fig.3a and the electric fields are shown in Fig.4. As we can see, even at the distance of z = -300nm (the central plane of the bottom cladding layer), one still has strong field, as well as in the central top cladding layer at a distance of 100nm away from the upper core boundary. This shows the large

mode profile spreading because of the weakly confined structure in the vertical direction.

Out-off plane scattering is evaluated by the same method, i.e., 2D cutting planes are selected to be parallel to *xy* plane and with a distance of 100nm away from the top and bottom of the structure. Our investigations have shown that there is no region parallel to the cladding layers with strong out-off-plane radiation (i.e., less than 2%), but there still is the *z* component of the Poynting vector above the cladding layer and this component is bigger than the vector below the bottom layer.

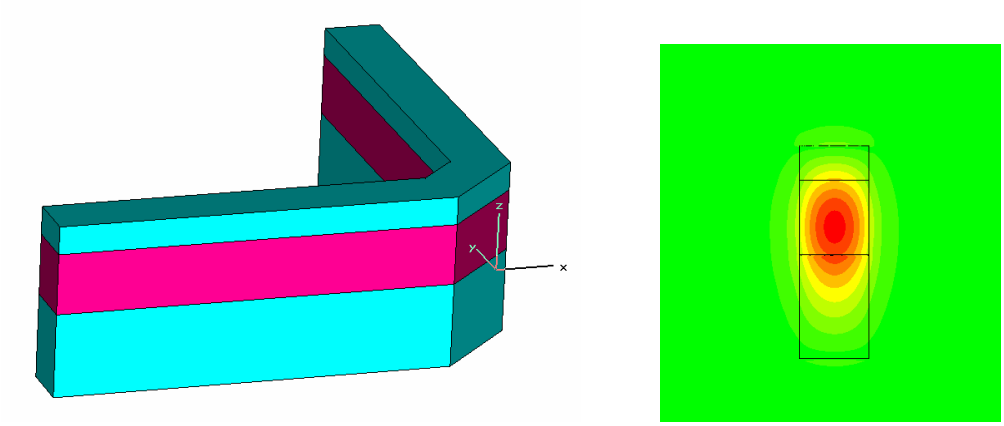

Fig.3: (a) The 3D trench waveguide bend structure used for calculation. The region in red is the core layer, while the regions in blue are top and bottom cladding layers, respectively. Note that z=0 is at the bottom of the core layer. (b) Eigenmode profile of the fundamental TM mode from the MWS eigenvalue solver; red color indicates high field values.

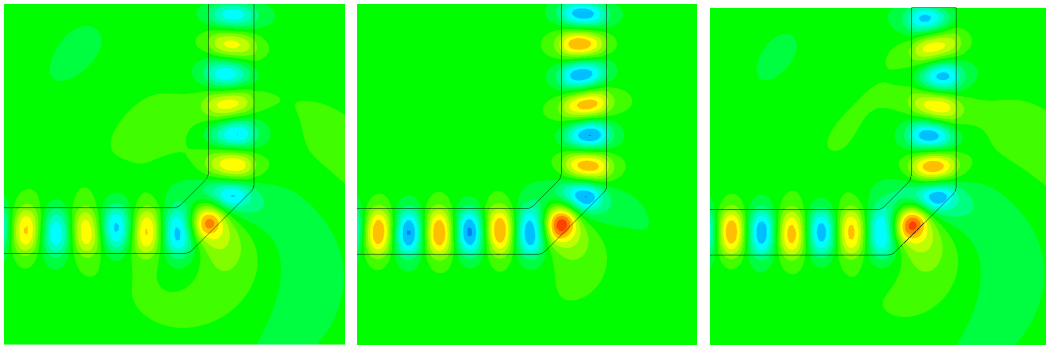

Fig.4: Field distribution Ez for different 2D cutting planes, which are in the central planes of the respective layers. (a) z = 534nm; (b)z = 217nm; (c) z = -300nm.

In the bend regions, a slightly stronger radiation is clearly visible especially in the outer bend region as indicated in Fig.4. This could be explained as follows: The trench structure with the 45 degree waveguide section is still not sufficiently well optimized. Some energy leaks out and results in radiation, as predicted from 2D simulations [1]. Furthermore, the mode mismatching mentioned above, may contribute to the radiation losses because the exact mode matching condition

of the bend geometry is violated.

Since direct optimization of the 3D structure is time-consuming, we have to go back to 2D modeling to find some promising topologies that could improve the bend performance. Our 2D simulations show that the transmission for the fundamental mode can be improved over a wide frequency range when local PhCs are present at the bend corners [1]. Here, the PhCs act as 'mirrors' or 'resonators' which could reflect or couple the radiation back into the waveguide. These two PhCs inside and outside the bend are designed in such a way that at least the operation wavelength of the waveguide is located within the first band gap of the PhCs. After positioning the PhCs near the bend, the structure looks as shown in Fig.5. The exact geometric parameters of this structure are given in [1]. The 3D simulation shows a very good agreement with 2D simulation although the transmission predicted by the 2D simulation is higher than in the 3D case. This is because of the finite size in the third dimension, off-plane loss, and higher reflection at the input port and mode mismatching in the 3D model. Fig.5b shows the field distribution at z = 217nm in a 2D plane for the fundamental mode at 1.55μm, reasonable propagation behavior is observed. Again, the same routines are used to check the out-off plane loss and the same behavior has been found. That is, the scattering loss mainly originates from the bend and PhCs parts. It should be pointed out that some differences are still present because the PhCs scatter light and there is a component of scattering in z direction. From Fig.5b, we can see that more PhC layers are needed to prevent in-plane scattering loss because two layers are not enough to form a photonic band gap (PBG) which enables reflection of the out-scattered light back into the waveguide.

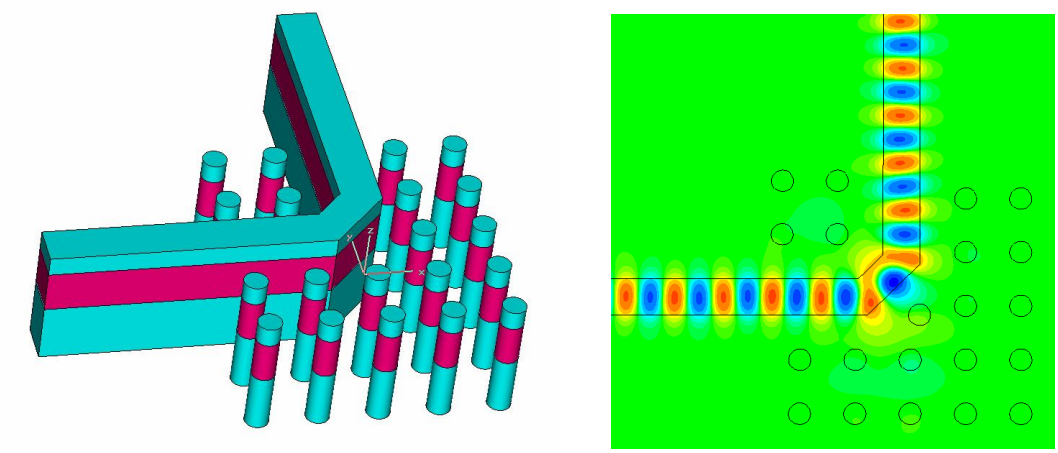

Fig.5: (a) 3D structure used for simulation when the PhCs are added on both sides of the bend; (b) Electric field at z = 217(the central plane of the core layer);

Besides the loss mechanisms mentioned above, substrate loss is another major concern in waveguide structures when the effective index of the mode is less than the index of the bottom cladding. As the mode is weakly confined in the vertical direction, a higher bottom cladding layer and high aspect ratio etching are required. When such a trench waveguide is designed, the trench has to be selected much higher than the height of the core [12]. In the calculation above, we did not take the substrate into account for the following reasons: The structure is deeply etched and sufficiently beneath the core, then the evanescent tail of the field is very small when it reaches the bulk cladding. Thus, substrate loss is on the acceptable level even though it is always present. A more direct but time-consuming method to evaluate the substrate

loss is using numerical mode solvers that can handle complex eigenvalue problems and to search for the complex propagation constants of the modes where the substrate loss is inherent to their imaginary part.

To partially check the fabrication tolerance with simulations, we also investigated the impact of structural variations. When the radii of PhC rods change from 110nm to 140nm, the transmission changes by only 1%. This may be understood from the fact that the operating wavelength of the structure is still within the band gap when the radii changes in this range. More detailed studies showed that the distance between the first PhC layer and the waveguide has a stronger impact than the radii of PhCs. An acceptable tolerance of the distance is 30nm. Also the most sensitive rod 'A' (see, Fig.4a in [1], the location of A is (200nm, -200nm)) plays an important role because its location must be more precise than others, typically within 50nm. From this sense, the photonic crystals are acting like resonators with relative low quality factors. Fig.6 shows the spectral response of the power transmission for the two cases when the PhCs are absent/present near the bend. The transmission is considerably improved within a wide band region when the PhCs are added. This means that the PhCs indeed help to improve the performance and partially solve some fabrication imperfection problems at the same time. This analysis agrees very well with the results predicted by the two dimensional simulation, although the transmission is lower than in the 2D simulation.

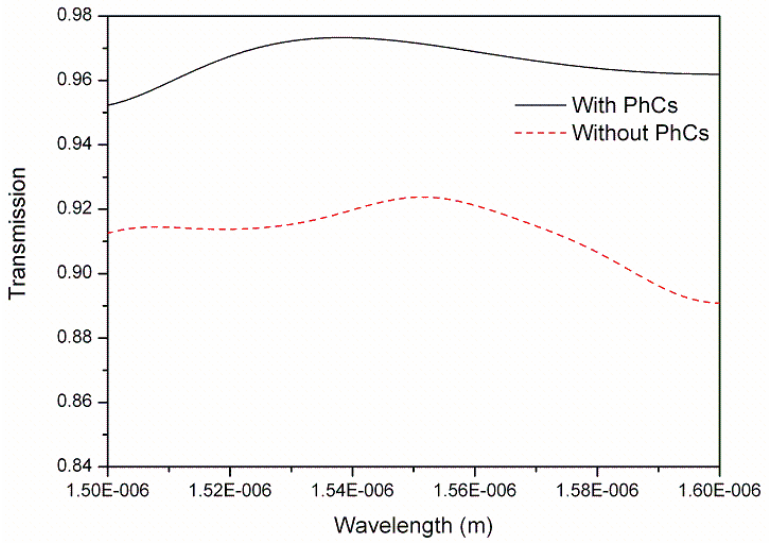

Fig. 6: 3D Simulation of the power transmission's spectral response for a bend with PhCs (solid line), and without PhCs (dashed line).

IV. COMPARATIVE STUDY WITH SILICON BASED MATERIAL SYSTEM

One of the advantages using silicon material system is that high index contrast can be obtained, i.e., vertical index contrast Δn is much larger than that InP can have. Therefore, the vertical wave confinement in the trench waveguide can be improved if such material systems are adopted [14]. To study the influence of the high vertical index contrast on the performance of trench waveguide, we simulated a new structure but with the same geometric parameters as we used before (cross-section geometry). The only difference is the cladding index that has changed to 1.5 and the core index that

is set to 3.5. The mode profile was calculated and we can see from Fig.7, the mode field is strongly confined in the core region compared to the InP trench waveguide shown in Fig.3. The same routine is then used to find the effective index and reused for optimization in MaX-1 platform [13] to get reasonable geometries. Our 2D simulations have shown that without optimizing the bend geometric parameters of the new structure, high transmission is still obtained when two 45 degree mirrors are introduced into the bend structure. The 2D results are still comparable between the two material systems with little variation but the 3D results show with large differences. This means that a slight variation of the 2D effective index causes pronounced effects and one has to go back to the initial configuration to search for an optimal bend topology. In other words, simple scaling rules failed for the sharp trench waveguide design. Since the mode fields are tightly confined in the core region, the out off plane loss are greatly reduced due to mode spread and substrate losses are then when the high index contrast material system was employed. While other behaviors such as out-off plane loss are held similarly to the InP material system, i.e., very low out-off plane loss is observed. The most notable exception is that the PhC parts need to be redesigned to meet the needs of "resonators and mirrors" behaviors because the higher indexes contrast between the core and cladding layers.

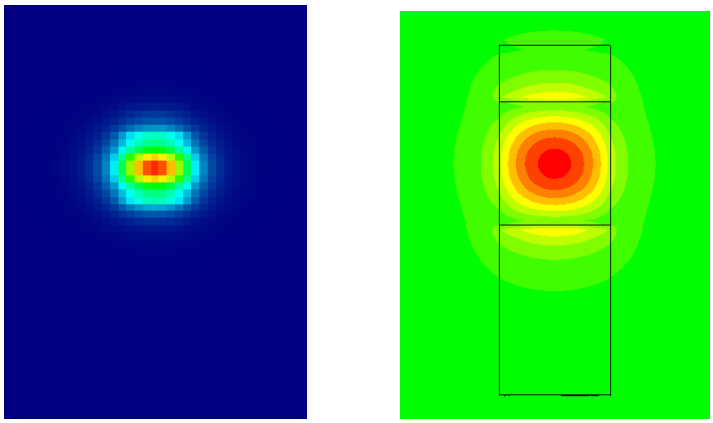

(a) (b)

Fig.7: Fundamental TM mode of the trench waveguide within the silicon material system; simulations are performed (a) with the Apollo eigenmode solver, and (b) with the MWS eigenmode solver.

Table 2: Calculated effective index from different eigenmode solvers for the fundamental TM mode of Silicon trench waveguide at 1.55 μm.

Eigenmode Solver	2D Effective index	1-D central slice effective index	1-D lateral slice effective index	Propagation Constant
Hammer EIM	2.735	3.248	1.000	13.160 μm^{-1}
Apollo	2.786	3.088	1.000	11.295 μm^{-1}
MWS	2.73	/	/	11.073 μm^{-1}

V. FABRICATION, MEASUREMENT AND CHARACTERIZATION

In order to experimentally validate the simulation results, we implemented the most reliable structure in an InP/InGaAsP/InP vertical slab waveguide using a combination of electron-beam lithography for patterning and inductively-coupled plasma reactive ion etching (ICP-RIE) of the core and cladding layers [15]. To estimate the propagation loss and to easily characterize the structure, two identical 90 degree bends for collinear in-and-out coupling separated by a 30μm straight waveguide were fabricated at the same time.

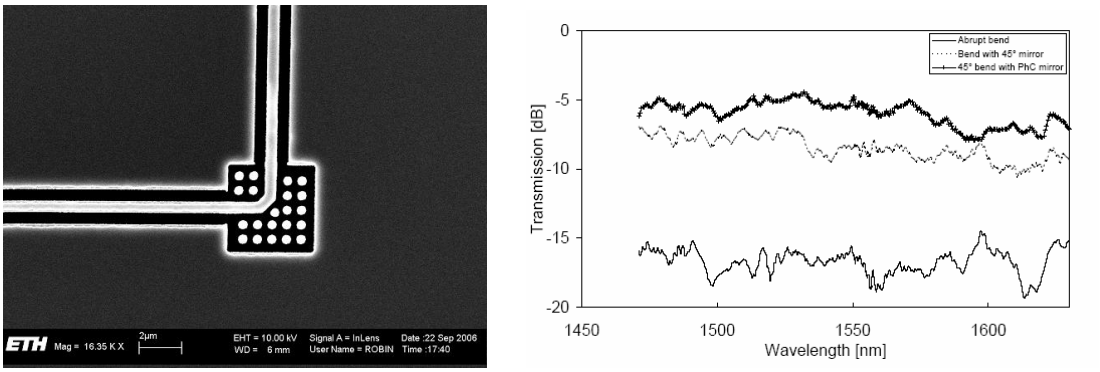

(a) (b)

Fig.8: (a) SEM picture of the fabricated structure; (b) Measured spectral responses of the power transmission for the three structures: Curves from top to bottom are: 45° mirror bend with PhCs, bend with 45° mirror, abrupt bend.

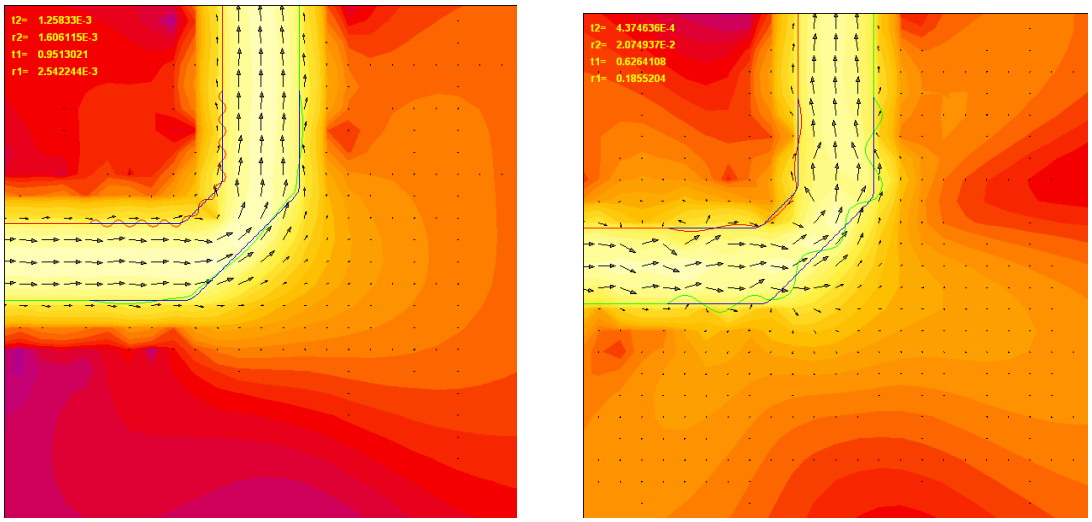

(a) (b)

Fig.9: Perturbation simulations for the waveguide's bending area. The boundaries with green and red color denote the perturbed waveguide boundaries where random periods are used. (a) The perturbation amplitude for the outer boundary is less than for the inner boundary, the transmission of the fundamental mode T1=0.95; (b) The perturbation amplitude for the outer boundary is larger than for the inner boundary, the transmission of the fundamental mode T1=0.62.

One straight waveguide was fabricated on the same chip as a reference waveguide to deembed the access-waveguide losses and will serve as a reference waveguide during measurements. A system based on end-fire technique was set up to measure the optical transmission. Two tunable lasers with span range 1465-1630nm were used, followed by a series of polarization controllers, combiners, and inline polarizers. One laser output was used for reference power measurement. The second laser was coupled to the device under test via a tapered lensed fiber. Since we just simulated the 3D structure for TM polarization (electric field is along Z direction as shown in Fig.5a), for comparison reasons, all the measurements are based on TM polarization and we didn't compare with TE case to investigate the polarization dependence of the structure. Additionally, 1.5mm-long and 1μm-wide access waveguides coupled the light in and out of the device by means of 15μm long tapering sections.

Fig.8a shows the SEM picture of the fabricated structure and Fig.8b shows the measured transmission through the double bends for different type bends after de-embedding of the access waveguides. As we expected from simulations, the measured transmission of the abrupt bend (i.e., without 45° mirror) is the lowest one with less than -15dB, the sum of losses and reflections amounts to ca.8dB/bend. Meanwhile, the bend with two 45° mirrors and additional PhC mirrors show losses and reflection of ca.4dB/bend and 2.5dB/bend, respectively. An improvement larger than that predicted by the simulation confirms the lower sensitivity of the bend with PhC mirror on fabrication imperfections. From Fig.8, we can see that the measured results agree very well with the simulation results although the maximum transmission values are not reached as the simulation shows. This can be explained as fabrication imperfections during process and misalignment during measurement. But it should point out that for the deeply etched structure, the imperfections mainly come of fabrication process, which is unavoidable in the deeply etched InP/Silicon material system.

In our case, the fabrication imperfections mainly show up as surface roughness, resulting in transmission loss that scales with the square of the roughness amplitude. Therefore new smoothing technique should be used to reduce the sidewall roughness, which is a major source of loss and a severe obstacle when realizing high transmission in trench waveguide whether the material system is. To numerically check the influence of sidewall roughness on the transmission of the waveguide, a perturbation with random periods was introduced to the bend part as shown in Fig.9. The results show that in general higher roughness amplitudes cause higher transmission loss although we didn't exclude that lower loss may still have.

VI. CONCLUSIONS

In this paper, we have presented 3D simulation of sharp trench waveguide bends that is extended by combining with a small PhC around the bending area. The methodology used here relies on optimizing the 90° waveguide bend by introducing two 45° mirrors to reduce the radiation loss as well as to redirect the mode propagation. The PhCs here act as mirrors and resonators and help improve the transmission and then solver few fabrication imperfections. The work we did here shows that three dimensional simulations can offer full insights into the structure's underlying behavior, which is not accessible with 2D modeling. Experimental results show a very good agreement with theoretical predictions. Higher index contrast material system has very well field confinement, thus low off-plane losses are obtained for the high index contrast structure. Since sidewall roughness is the major source of scattering losses in trench waveguide, new fabrication process is expected to be developed to overcome the difficulties in the near future. We have to point out here that although waveguide bends are conceptually simple, waveguide fabrication is still complicated by the need of

material and on-chip compatibility requirements, as well as design and simulation. Hopefully, our designs would bring us steps close to the realization of high density optical circuit components.

ACKNOWLEDGEMENTS

This work was supported by research grants of the ETH Zurich and of the Swiss National Science Foundation. Device fabrication was performed in the framework of the Nanostructuring platform of the European ePiXnet network of excellence on photonic integrated circuits.

REFERENCES

1. Cui Xudong, Christian Hafner, Ruediger Vahldieck, Franck Robin, *Opt. Express*, **14**, 4351-4356, (2006).
2. H. F. Taylor, *Appl. Opt.*, **16**, 3, 711-716, (1977).
3. C. Manolatou, Steven G. Johnson, Shanhui Fan, Pierre R. Villeneuve, H. A. Haus, and J. D. Joannopoulos, *J. lightwave Technol.,* **17**, 1682-1692, (1999).
4. Andrea Melloni, Federico Carniel, Raffaella costa, and Mario Martinelli, *J. Lightwave Technol*. **19**, 571-577, (2001).
5. R.L. Espinola, R.U. Ahmad, F. Pizzuto, M. J. Steel and R.M. Osgood, Jr. *Opt. Express*, **8**, 517-528, (2001).
6. Andrea Melloni, Paolo Monguzzi, Raffaella Costa, and Mario Martinelli, *J. Opt. Soc. Am. A*, **20**, 130-137, (2003).
7. A. Mekis, J. C. Chen, I. Kurland, S. Fan, P. R. Villeneuve, and J. D. Joannopoulos, *Phys. Rev. Lett,*. **77**, 3787, (1996).
8. http://wwwhome.math.utwente.nl/~hammer/eims.html.
9. A. Kumar, K. Thyayarajan, and A. K. Ghatak, *Opt. Lett.*, **8**, 63-65, (1983).
10. C. M. Kim, B. G. Jung, and C. W. Lee, *Electron. Lett.*, 22, 296-298, (1986).
11. www.apollo.com.
12. www.cst.com.
13. http://alphard.ethz.ch/max-1.html.
14. Milos Popovic, Kazumi Wada, Shoji Akiyama, Hermann A. Haus, Juergen Michel, *J. lightwave technol.*, **20**, 1762-1772 ,(2002).
15. Franck Robin, Ping Ma, Patric Strasser, Robert Wuest, Heinz Jaeckel, Cui Xudong, Christian Hafner, in the *1st European Topical Meeting on Nanophotonics and Metamaterials*, Seefeld ski resort, Tirol, Austria, 8-11 January, (2007).